RESEARCH ARTICLE

Electronic Structure, Optical and Thermoelectric Properties of Li_2AgSbX_6 (X = F, Cl, Br, I) Double Perovskites

Seema Gul[1] **and Amir Sohail**[1,*]

[1] Department of Physics, Abdul Wali Khan University, Mardan 23200, Pakistan

Abstract

Halide double perovskites offer wide compositional flexibility and are being explored for energy-related applications. In this work, the structural, electronic, optical, and thermoelectric properties of Li_2AgSbX_6 (X = F, Cl, Br, I) were investigated using density functional theory (DFT) within the WIEN2k package. Structural optimization shows a systematic increase in lattice parameter from F → I, accompanied by a decrease in bulk modulus, indicating higher compressibility for the heavier-halide compounds. Electronic-structure calculations within PBE-GGA identify all compositions as indirect-gap semiconductors, with band gaps decreasing across the series: 1.599 eV (F), 1.389 eV (Cl), 0.509 eV (Br), and 0.307 eV (I). Density-of-states analysis indicates that the valence band is dominated mainly by Ag and halogen states, while the conduction band is largely governed by Li and Sb contributions. Optical spectra derived from the calculated electronic structure (dielectric function and related optical constants) show strong optical activity and absorption spanning the visible-to-UV range, with the response shifting to lower photon energies for heavier halides. Thermoelectric transport coefficients were evaluated using BoltzTraP within the constant relaxation-time framework (σ/τ, κ_e/τ, S, and $S^2\sigma/\tau$), and the reported ZT trend indicates that $Li_2AgSbCl_6$ exhibits the most favorable and temperature-stable thermoelectric performance in the presented dataset ($ZT \approx 1$), whereas the I-based compound shows a pronounced reduction at elevated temperature. The Seebeck trends indicate p-type behavior for Li_2AgSbF_6 and $Li_2AgSbBr_6$ and n-type behavior for $Li_2AgSbCl_6$ and Li_2AgSbI_6 under the adopted transport conditions.

Keywords: double perovskites, electronic properties, thermoelectric properties, optoelectronics.

1 Introduction

Perovskites have become central to materials research, particularly for solar-energy conversion, because they can be prepared by relatively simple routes and show strong optoelectronic response. Halide perovskites are now explored in solar cells, LEDs, coatings, and memory devices. A key attraction is their tolerance to certain defects while maintaining useful electronic

Submitted: 20 February 2026
Accepted: 27 February 2026
Published: 28 February 2026

Vol. 2, **No.** 1, 2026.
10.62762/JAEM.2026.936533

***Corresponding author:**
✉ Amir Sohail
Amirsohail305@gmail.com

Citation
Gul, S., & Sohail, A. (2026). Electronic Structure, Optical and Thermoelectric Properties of Li_2AgSbX_6 (X = F, Cl, Br, I) Double Perovskites. *Journal of Advanced Electronic Materials*, 2(1), 1–7.

and optical performance. Many compositions show strong light absorption and efficient carrier transport, and the efficiency of metal-halide perovskite solar cells has continued to improve [1–3].

Double perovskites extend the conventional perovskite framework (ABX_3) by replacing the single divalent B-site cation with two different cations, typically a monovalent ion (B^+) and a trivalent ion (B^{3+}), giving the general formula $A_2B'B''X_6$ [4]. The structure is built from corner-sharing BX_6 octahedra, and the B′/B″ sublattice can adopt an ordered arrangement. Because their properties depend strongly on composition, double perovskites are frequently assessed using density functional theory (DFT), including structure, electronic bands, optical response, and thermoelectric indicators. Recent interest has also focused on inorganic Bi-based double perovskites such as $Cs_2AgBiCl_6$ and $Cs_2AgBiBr_6$, where the band-gap values motivate study but may be less favorable for certain optoelectronic applications [5, 6].

Motivated by these developments, we focus here on Li_2AgSbX_6 (X = F, Cl, Br, I). Previous work on Li_2AgSbX_6 with X = Cl, Br, and I reported indirect semiconducting gaps of 1.40 eV (Cl), 1.00 eV (Br), and 0.40 eV (I), along with strong absorption and thermoelectric trends linked to low thermal conductivity and a high power factor at low temperature [7]. In this project, we provide a systematic study of the structural, electronic, optical, and thermoelectric properties of Li_2AgSbX_6 across the full halide series (X = F, Cl, Br, I) using the FP-LAPW method implemented in the WIEN2k package.

2 Computational Methodology

All calculations were carried out within density functional theory (DFT) using the all-electron full-potential linearized augmented plane-wave (FP-LAPW) method as implemented in the WIEN2k package [11]. In this approach, the unit cell is divided into non-overlapping muffin-tin spheres centered on the atoms and an interstitial region. The wave functions are expanded into atomic-like functions inside the spheres and in plane waves in the interstitial region, which allows an accurate treatment of bonding and electronic structure without shape approximations to the potential. The exchange–correlation energy was treated using the Perdew–Burke–Ernzerhof generalized gradient approximation (PBE-GGA) throughout this work. Self-consistent field (SCF) cycles were iterated until the total energy converged to 10^{-5} Ry and the charge density converged to 10^{-4} e. These thresholds were adopted to ensure that the structural trends and derived electronic/optical/transport quantities were numerically stable.

3 Results and Discussion

In the double perovskite halides Li_2AgSbX_6 (X = F, Cl, Br, I), the A site is occupied by Li^+, whereas the B site is occupied by two different cations (Ag and Sb). Each B-site cation is coordinated by six halide anions (F^-, Cl^-, Br^-, I^-), forming BX_6 octahedra. These octahedra are connected through corner sharing, which builds the three-dimensional double-perovskite framework. To accommodate ionic-size effects and maintain structural stability, octahedral tilting may occur. On the B sublattice, Ag and Sb are arranged in an ordered rock-salt (NaCl-type) pattern. The compounds investigated crystallize in the cubic structure with space group Fm-3m (No. 225). Structural details are listed in Table 1. Each compound reaches its lowest energy (E_0) at the equilibrium volume, corresponding to the most stable configuration. As the halogen changes from F to I, the equilibrium volume increases, and the total energy becomes more negative, consistent with the larger size of I. The lattice parameter a_0 increases from F to I, following the Shannon radii trend [8]. The larger a_0 of Li_2AgSbI_6 relative to the other three compounds is attributed to the larger size of I. The lower bulk modulus of the I-based compound supports the inverse relation between lattice constant and bulk modulus: as the lattice constant increases, bonding weakens and compressibility increases, resulting in a smaller bulk modulus [7]. Structural parameters obtained using the Birch–Murnaghan equation of state are listed in Table 1.

To assess thermodynamic stability, the formation energy (ΔH_f) was calculated using the following expression:

$$\Delta H_f = E_{\text{Total}}(\text{Li}_m\text{Ag}_m\text{Sb}_n\text{X}_o) - mE_{\text{Li}} - mE_{\text{Ag}} - nE_{\text{Sb}} - oE_{\text{X}}$$

Here, the elemental energies of Li, Ag, Sb, and X ($E_{\text{Li}}, E_{\text{Ag}}, E_{\text{Sb}}, E_{\text{X}}$) are subtracted from the total energy of the compound (E_{Total}). The calculated formation energies are negative for these double perovskites, indicating that the compounds are thermodynamically stable.

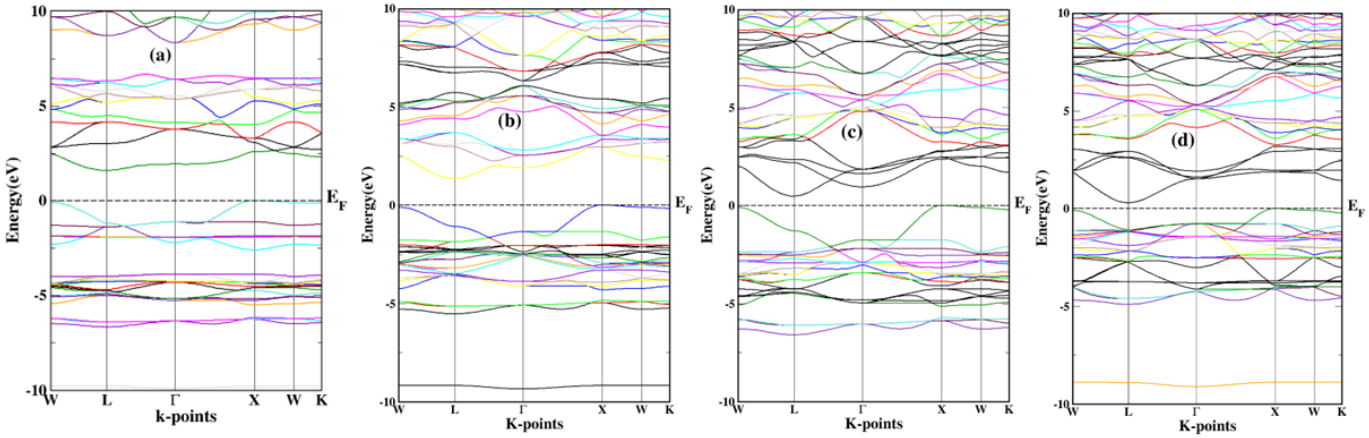

Figure 1. Band structures of (a) Li_2AgSbF_6, (b) $Li_2AgSbCl_6$, (c) $Li_2AgSbBr_6$, and (d) Li_2AgSbI_6.

Table 1. Lattice parameter (a_0), ground-state volume (V_0), bulk modulus (B), pressure derivative of bulk modulus (BP), ground-state energy (E_0), and formation energy ΔH_f.

Compound	a_0 (Å)	a_0 (Bohr)	V_0 (Bohr)	B (GPA)	BP	E_0 (RY)	ΔH_f eV/atom
Li_2AgSbF_6	9.18	17.31	1298.37	47.32	4.8084	-24830.94	-32.29
$Li_2AgSbCl_6$	10.50	20.31	2094.056	28.41	3.9513	-29170.62	-25.07
$Li_2AgSbBr_6$	10.70	20.33	2100.48	27.278	4.7660	-29170.61	-2.9
Li_2AgSbI_6	11.94	22.56	2873.72	20.312	5.5910	-109060.9	-1.189

Li_2AgSbX_6 (X = F, Cl, Br, I) exhibits an indirect semiconducting band gap, because the conduction-band minimum lies above the Fermi level and the valence-band maximum lies below it, and these extrema occur at different k-points ($X - L$), as shown in Figure 1. From the present calculations, the band gaps of Li_2AgSbF_6, $Li_2AgSbCl_6$, $Li_2AgSbBr_6$, and Li_2AgSbI_6 are 1.599, 1.389, 0.509, and 0.307 eV, respectively. The band gap decreases systematically from F to I, which is consistent with the increasing ionic radius of the halide ion: larger halide ions increase orbital overlap and reduce the gap. This

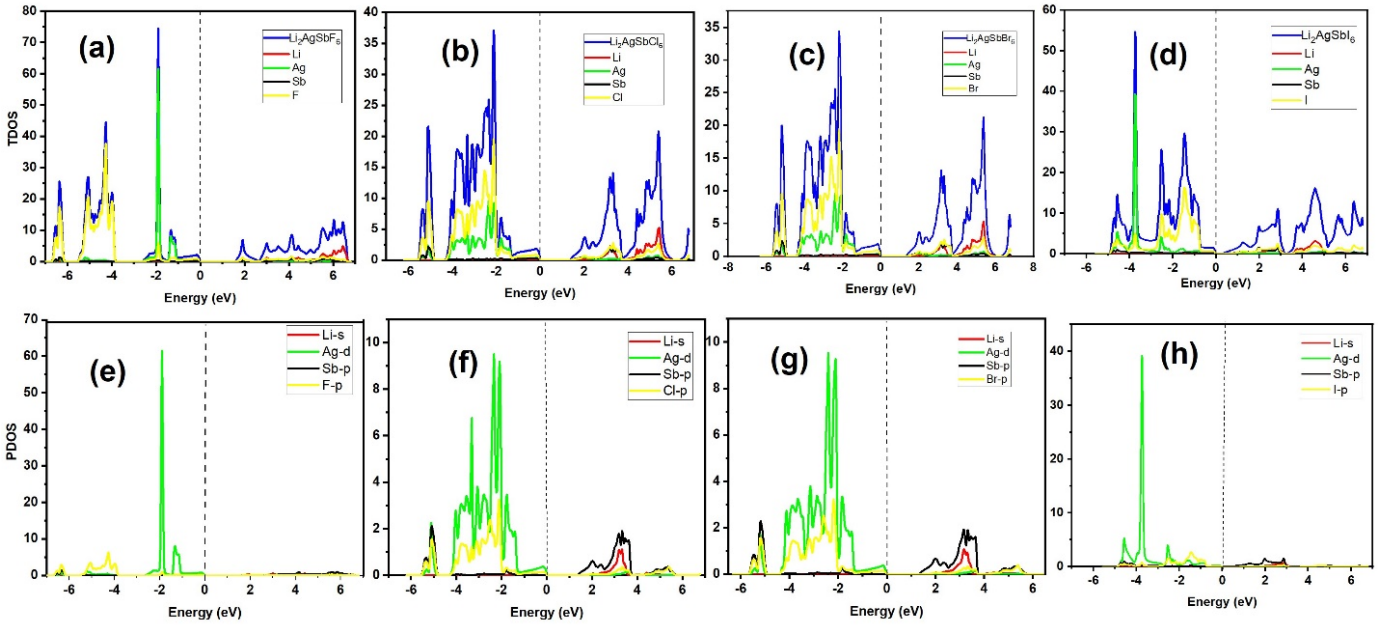

Figure 2. TDOS of (a) Li_2AgSbF_6, (b) $Li_2AgSbCl_6$, (c) $Li_2AgSbBr_6$, and (d) Li_2AgSbI_6, and PDOS of (e) Li_2AgSbF_6, (f) $Li_2AgSbCl_6$, (g) $Li_2AgSbBr_6$, and (h) Li_2AgSbI_6.

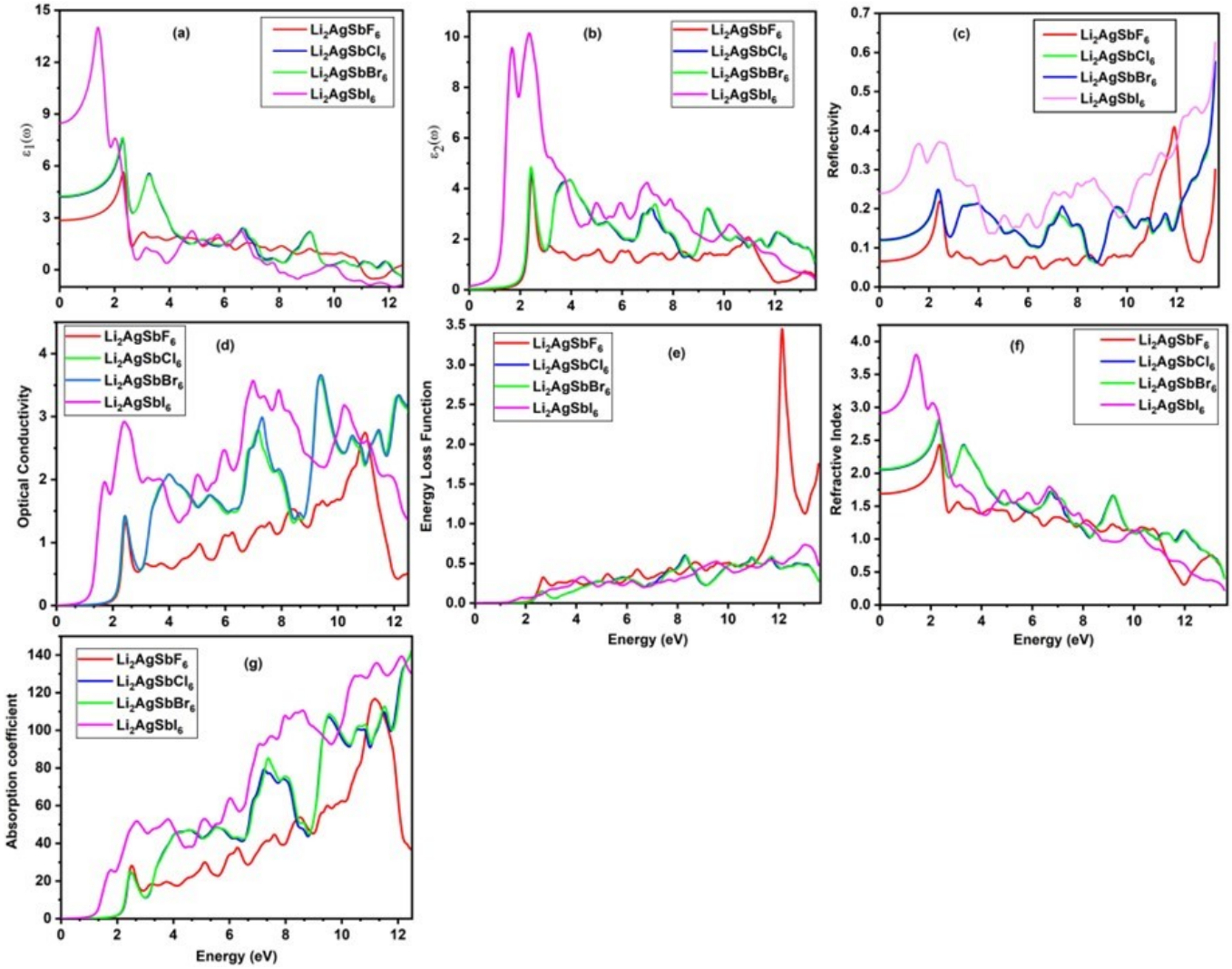

Figure 3. Optical spectra of Li_2AgSbX_6 (X = F, Cl, Br, I): (a) $\varepsilon_1(\omega)$, (b) $\varepsilon_2(\omega)$, (c) reflectivity, (d) optical conductivity, (e) energy-loss function, (f) refractive index, and (g) absorption coefficient.

halide substitution therefore modifies the band gap and, consequently, influences the optical response and transport behavior, which is relevant for solar-cell applications [9].

The density of states (DOS) describes the number of available electronic states as a function of energy and helps in interpreting electronic transport and bonding features. The total DOS (TDOS) of Li_2AgSbX_6 (X = F, Cl, Br, I) was calculated using the PBE-GGA functional and is plotted versus energy in Figure 2. The dashed line marks the Fermi level, fixed at 0 eV, which separates the valence-band and conduction-band regions. In all cases, the DOS does not cross the Fermi level, confirming the semiconducting nature of these compounds. The TDOS shows the overall contribution of all atoms to the valence and conduction regions, whereas the partial density of states (PDOS) resolves the orbital contributions of individual atoms. From the TDOS and PDOS results, the valence band is mainly formed by Ag and the halogen atoms (F, Cl, Br, and I). In the conduction band, particularly within the 2–4 eV energy range above the Fermi level, the larger contributions come from Li and Sb states. The halogen atoms also show some participation in this region, but their contribution is comparatively smaller. This can be clearly seen in Figure 2(e–h). In the PDOS, Ag-d and halogen p states contribute strongly to the valence band, whereas Li-s and Sb-p states contribute strongly to the conduction band. When the halogen is changed from F to I, the separation between valence and conduction-band features narrows, and the DOS shifts closer to the Fermi level, consistent with the reduced band gap and in agreement with the band-structure trends [7].

Optical properties describe how a material responds to electromagnetic radiation and are therefore relevant

for optoelectronic and solar-energy applications. For Li_2AgSbX_6 (X = F, Cl, Br, I), the optical response is presented in terms of the complex dielectric function, $\varepsilon(\omega) = \varepsilon_1(\omega) + i\varepsilon_2(\omega)$, and the derived optical constants (Figure 3). The real part $\varepsilon_1(\omega)$ (Figure 3(a)) reflects the polarization response, while the imaginary part $\varepsilon_2(\omega)$ (Figure 3(b)) represents interband absorption. In the low-energy region, the I-based compound exhibits the largest dielectric response (a pronounced maximum around ∼1–2 eV), whereas the F-based compound shows the smallest overall magnitude, consistent with the stronger low-energy optical activity of the heavier halide. The same trend is reflected in the reflectivity (Figure 3(c)), Li_2AgSbI_6 starts with the highest low-energy reflectivity and rises strongly again toward the high-energy end of the plotted range (approaching ∼0.6–0.65 near 14 eV), while the other compositions remain lower. Importantly, reflectivity here is plotted as a fraction (not percent). Overall, the systematic shift of optical onset features to lower photon energy from F → I is consistent with the decreasing band gap across the series, i.e., heavier halides support stronger response at lower photon energies [10].

The optical conductivity (Figure 3(d)) shows where interband transitions contribute most strongly to the optical response; the dominant structures occur broadly in the mid-energy range (∼7–11 eV), with Li_2AgSbI_6 showing strong intensity at comparatively lower energies than Li_2AgSbF_6. The energy-loss function $L(\omega)$ (Figure 3(e)), which highlights plasmon-like loss features, remains relatively small for Cl/Br/I over most of the range but shows a pronounced high-energy resonance for the F-based compound near ∼12–13 eV; this should be stated explicitly because it is a distinctive feature of the plotted spectra. The refractive index $n(\omega)$ (Figure 3(f)) is highest at low photon energies for Li_2AgSbI_6 (approaching ∼3.5–3.8 near ∼1 eV), while Li_2AgSbF_6 is the lowest (∼1.6–2 in the same region), and all compositions decrease gradually with energy as dispersion weakens. Finally, the absorption (Figure 3(g)) increases with photon energy for all compounds, with Li_2AgSbI_6 exhibiting the strongest low-energy absorption and Li_2AgSbF_6 the weakest, consistent with the band-gap trend. Thus, overall optical characteristics suggest the suitability of these materials for optoelectronic applications.

Thermoelectric transport for Li_2AgSbX_6 (X = F, Cl, Br, I) was evaluated using Boltzmann transport theory (BoltzTraP) within the constant relaxation-time approximation, so the conductivity and electronic thermal conductivity are presented in the scaled forms σ/τ and κ_e/τ. Figure 4(a) shows that σ/τ increases with temperature for all compositions, consistent with thermally activated transport in semiconducting systems. $Li_2AgSbBr_6$ exhibits the largest σ/τ throughout the range (reaching $\sim 8.5 \times 10^{18}\,\Omega^{-1}\,m^{-1}\,s^{-1}$ at the upper end of the plotted temperatures), while $Li_2AgSbCl_6$ remains much smaller and close to the baseline. The Seebeck coefficient in Figure 4(b) is positive for Li_2AgSbF_6 and $Li_2AgSbBr_6$ and negative for $Li_2AgSbCl_6$ and Li_2AgSbI_6, indicating p-type and n-type tendencies, respectively, under the chemical-potential conditions used in the calculation. In all cases, $|S|$ decreases with temperature, with very large magnitudes at low temperature (order $10^3\,\mu V/K$ on the plotted scale) that relax toward smaller values at higher temperature.

Figure 4(c) shows that the electronic thermal conductivity term increases with temperature for all compositions, and the ordering largely follows σ/τ. $Li_2AgSbBr_6$ is the highest, while $Li_2AgSbCl_6$ remains the lowest. The power factor in Figure 4(d), plotted as PF = $S^2\sigma/\tau$, is strongly enhanced for $Li_2AgSbBr_6$ and rises steeply with temperature, whereas Li_2AgSbI_6 shows a more moderate PF that increases up to mid-T and then slightly decreases at higher temperature. Li_2AgSbF_6 rises slowly, and $Li_2AgSbCl_6$ stays comparatively small. The combined effect appears in the figure of merit, Figure 4(e), $Li_2AgSbCl_6$ maintains the highest and most stable ZT (near ∼0.95–1.0 over the plotted range), followed by Li_2AgSbF_6 (gradual decrease toward ∼0.9). $Li_2AgSbBr_6$ drops from ∼0.9 at low temperature toward ∼0.75 at high temperature, while Li_2AgSbI_6 shows a pronounced degradation with temperature, falling to ∼0.1 by ∼800–850 K. Overall, the figure shows that halide substitution strongly tunes σ/τ, κ_e/τ, PF, and ZT, with Cl giving the most temperature-stable ZT in this dataset and I showing the weakest high-temperature ZT behavior. It should be noted that the calculated ZT values include only the electronic contribution to thermal conductivity; therefore, they represent upper-limit estimates. Additionally, these materials possess a higher ZT value than several other reported similar double perovskites, such as $Cs_2AgBiCl_6$ (0.72), $Cs_2AgBiBr_6$ (0.71) [12], $Cs_2AgSbCl_6$ (0.72), and $Cs_2AgSbBr_6$ (0.73) [13], $In_2AgSbCl_6$ (0.75), $In_2AgSbBr_6$ (0.77), and In_2AgSbI_6 (0.76) at 300 K [10].

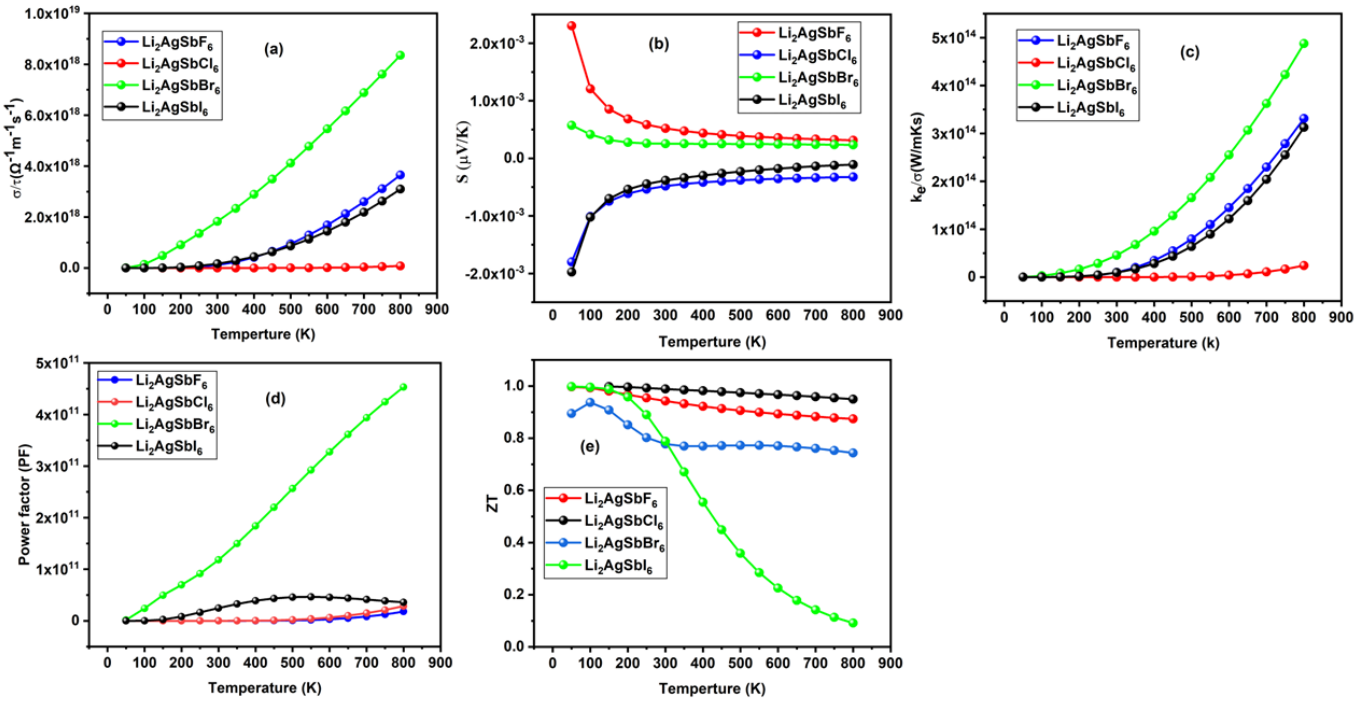

Figure 4. (a) Electrical conductivity, (b) Seebeck coefficient (S), (c) thermal conductivity, (d) power factor, and (e) Figure of merit (ZT) for Li_2AgSbX_6 (X = F, Cl, Br, I).

4 Conclusion

In this work, the structural, electronic, optical, and thermoelectric properties of Li_2AgSbX_6 (X = F, Cl, Br, I) double perovskites were investigated using DFT within the WIEN2k package. Structural optimization was performed using PBE-GGA, and the equilibrium lattice parameter, bulk modulus, and its pressure derivative were obtained by fitting the Birch–Murnaghan equation of state; the lattice parameter increases from F → I while the bulk modulus decreases, indicating higher compressibility for the heavier-halide compounds. Electronic-structure calculations (PBE-GGA) show that all compositions are indirect-gap semiconductors, with the band gap decreasing across the series: Li_2AgSbF_6 (1.599 eV), $Li_2AgSbCl_6$ (1.389 eV), $Li_2AgSbBr_6$ (0.509 eV), and Li_2AgSbI_6 (0.307 eV); TDOS/PDOS analysis indicates that the valence band is dominated by Ag and halogen states, whereas the conduction band is mainly contributed by Li and Sb (with Ag-d/halogen-p character in the valence region and Li-s/Sb-p character in the conduction region). Optical spectra derived from the PBE-GGA electronic structure (dielectric function, reflectivity, optical conductivity, energy-loss function, refractive index, and absorption) indicate strong optical activity with absorption extending from the visible into the UV range, with the I-based compound showing the largest low-energy dielectric and refractive response in the presented dataset. Thermoelectric transport coefficients computed using BoltzTraP (reported as σ/τ, κ_e/τ, S, and $S^2\sigma/\tau$) show clear halide-dependent trends; the plotted ZT behavior identifies $Li_2AgSbCl_6$ as the most temperature-stable and highest-performing composition (remaining near ∼1 over the shown range), while Li_2AgSbI_6 exhibits a pronounced reduction of ZT at elevated temperature. The Seebeck trends indicate p-type behavior for Li_2AgSbF_6 and $Li_2AgSbBr_6$, and n-type behavior for $Li_2AgSbCl_6$ and Li_2AgSbI_6, within the conditions used in the transport calculations. These results highlight their strong potential for practical applications in optoelectronic and energy-conversion devices, warranting further experimental validation and device-level exploration.

Data Availability Statement

Data will be made available on request.

Funding

This work was supported without any funding.

Conflicts of Interest

The authors declare no conflicts of interest.

AI Use Statement

The authors declare that no generative AI was used in the preparation of this manuscript.

Ethical Approval and Consent to Participate

Not applicable.

References

[1] Smestad, G., & Ries, H. (1992). Luminescence and current-voltage characteristics of solar cells and optoelectronic devices. *Solar Energy Materials and Solar Cells, 25*(1-2), 51-71. [CrossRef]

[2] Zhang, L., Mei, L., Wang, K., Lv, Y., Zhang, S., Lian, Y., ... & Ding, L. (2023). Advances in the application of perovskite materials. *Nano-Micro Letters, 15*(1), 177. [CrossRef]

[3] Loi, M. A., & Hummelen, J. C. (2013). Hybrid solar cells: perovskites under the sun. *Nature materials, 12*(12), 1087-1089. [CrossRef]

[4] Dai, J., Ma, L., Ju, M., Huang, J., & Zeng, X. C. (2017). In-and Ga-based inorganic double perovskites with direct bandgaps for photovoltaic applications. *Physical Chemistry Chemical Physics, 19*(32), 21691-21695. [CrossRef]

[5] Slavney, A. H., Hu, T., Lindenberg, A. M., & Karunadasa, H. I. (2016). A bismuth-halide double perovskite with long carrier recombination lifetime for photovoltaic applications. *Journal of the American chemical society, 138*(7), 2138-2141. [CrossRef]

[6] Wei, F., Deng, Z., Sun, S., Xie, F., Kieslich, G., Evans, D. M., ... & Cheetham, A. K. (2016). The synthesis, structure and electronic properties of a lead-free hybrid inorganic–organic double perovskite (MA) 2 KBiCl 6 (MA= methylammonium). *Materials Horizons, 3*(4), 328-332. [CrossRef]

[7] Nazir, S., Ayyaz, A., Alshihri, A. A., Zayed, O., Al-Daraghmeh, T. M., Alqorashi, A. K., ... & Mahmood, Q. (2024). Study of Mechanical, Optoelectronic, and thermoelectric aspects of lithium-based double perovskites Li2AgSbX6 (X= Cl, Br, I) for energy harvesting applications. *Materials Science and Engineering: B, 309*, 117651. [CrossRef]

[8] Harbi, A., Bouhmaidi, S., Pingak, R. K., Setti, L., & Moutaabbid, M. (2023). First-principles calculations to investigate optoelectronic, thermoelectric and elastic properties of novel lead-free halide perovskites CsRbPtX6 (X= Cl, Br and I) compounds for solar cells applications. *Physica B: Condensed Matter, 668*, 415242. [CrossRef]

[9] Ayyaz, A., Alkhaldi, H. D., Almashnowi, M. Y., Sfina, N., Anbarasan, R., Mera, A., & Mahmood, Q. (2024). Revealing elastic, thermophysical, optoelectronic, and transport characteristics of halide double perovskites Na2TlSbZ6 (Z= Cl/Br/I) for eco-friendly technologies: DFT analysis. *Inorganic Chemistry Communications, 170*, 113220. [CrossRef]

[10] Ayyaz, A., Zaman, M., Alkhaldi, H. D., Ali, H. I., Boukhris, I., Bouzgarrou, S., Al-Anazy, M. M., & Mahmood, Q. (2025). Computational screening of appealing perspectives of indium-based halide double perovskites In2AgSbX6 (X= Cl, Br, and I) for energy harvesting technologies. *RSC Advances*, *15*(15), 11128-11145. [CrossRef]

[11] Blaha, P., Schwarz, K., Tran, F., Laskowski, R., Madsen, G. K. H., & Marks, L. D. (2020). WIEN2k: An APW+lo program for calculating the properties of solids. *Journal of Chemical Physics, 152*(7), 074101. [CrossRef]

[12] Alotaibi, N. H., Mustafa, G. M., Kattan, N. A., Mahmood, Q., Albalawi, H., Morsi, M., Somaily, H. H., Hafez, M. A., Mahmoud, H. I., & Amin, M. A. (2022). DFT study of double perovskites Cs2AgBiX6 (X= Cl, Br): an alternative of hybrid perovskites. *Journal of Solid State Chemistry*, *313*, 123353. [CrossRef]

[13] Sajjad, A., Faizan, M., Alrebdi, T. A., Murtaza, G., Rehman, J., Shen, X., ... & Khan, S. H. (2025). Exploring double perovskites Cs 2 AgSbX 6 (X= Cl, Br, and I) as promising optoelectronic and thermoelectric materials: a first-principles study. *Physical Chemistry Chemical Physics, 27*(9), 4880-4891. [CrossRef]

Seema Gul recently completed her MPhil in Physics from the Department of Physics at Abdul Wali Khan University, Mardan. Her research specialization lies in Computational Materials Science, where she focuses on the theoretical and computational investigation of material properties using first-principles methods. Her academic work primarily involves density functional theory (DFT)–based simulations to study the structural, electronic, mechanical, and optical properties of advanced materials. She is particularly interested in modeling semiconductors and functional materials for potential applications in energy, electronics, and emerging technologies. (Email: seema.lfmd@gmail.com)

Amir Sohail completed his MPhil in Physics from the Department of Physics at Abdul Wali Khan University, Mardan, and is currently enrolled in the PhD program at the same institution. His research area is Computational Materials Science, with a focus on first-principles calculations and density functional theory (DFT) to investigate the structural, electronic, mechanical, and optical properties of advanced materials. His work emphasizes the theoretical design and characterization of functional materials for applications in energy storage, optoelectronics, and emerging technologies. (Email: amirsohail305@gmail.com)